Contemporary Mathematics
https://ojs.wiserpub.com/index.php/CM/

Research Article

A Social-Hydrological Framework for Assessing Irrigation Demand in Malawi: Linking Rainfall Variability and Poverty Dynamics

Tichaona Chikore[1], **Farai Nyabadza**[1,2*]

[1] Department of Mathematics and Applied Mathematics, University of Johannesburg, Auckland Park, Johannesburg, 2006, South Africa
[2] Institute of Research and Professional Training, Emirates Aviation University, Dubai International Academic City, P.O. Box 53044, UAE
E-mail: fnyabadza@uj.ac.za

Received: 20 June 2025; **Revised:** 4 August 2025; **Accepted:** 19 August 2025

Abstract: Malawi is an agrarian country highly dependent on rain-fed agriculture located in the Sub-Saharan Africa region which is characterized by a highly variable climate. This study presents a novel quantitative framework for assessing irrigation demand in Malawi by integrating climatic variability with socio-economic vulnerability over the period 2002 to 2022. Recognizing that irrigation needs stem not only from rainfall deficits but also from their socio-economic impacts we analyze annual segments capturing environmental and social conditions. Using normalized rainfall and poverty data we establish baselines representing optimal hydrological conditions and minimal social stress (using poverty as a proxy). We define hydrological stress as deviations from maximum rainfall and social stress as deviations from minimum poverty. These deviation metrics are combined into an irrigation need index which captures the compounded impact of water scarcity and poverty. The core of the methodology is an irrigation need index that integrates these stresses amplifying demand during years marked by significant rainfall shortfalls and elevated poverty. To capture temporal dynamics more effectively we interpolate the discrete index into a continuous function enabling the calculation of cumulative irrigation burden and average annual demand. The framework also identifies periods where irrigation need exceeds a critical threshold highlighting years of intensified stress. Key findings reveal an increase in irrigation need between 2020 and 2022 aligning with observed climate and poverty trends. This socially grounded data-driven approach provides a dynamic and policy-relevant tool for diagnosing irrigation urgency supporting more targeted equitable and timely water resource management strategies in Malawi.

***Keywords*:** irrigation demand, rainfall variability, poverty outcomes, hydrological stress, irrigation index, exceedance

MSC: 37N40, 91B74

1. Introduction

The intricate relationship between climate variability and socio-economic well-being is a pervasive challenge, particularly in agrarian economies highly dependent on natural resources [1]. Sub-Saharan Africa (SSA) in particular, frequently grapples with the cascading effects of unpredictable rainfall patterns, which directly impact agricultural productivity, food security, and ultimately, poverty levels [2, 3]. Historical data across the region consistently illustrate

DOI: https://doi.org/10.37256/cm.7120267539

how periods of drought or erratic rainfall exacerbate existing vulnerabilities, pushing already marginalized communities deeper into destitution. Efforts to mitigate these impacts have often centered on irrigation systems, recognized as a critical tool for buffering agricultural output against climatic shocks [4–6]. However, the effectiveness of irrigation interventions hinges not just on their technical feasibility, but on their strategic deployment in areas and times of genuine need [7]. This necessitates a comprehensive understanding of not only hydrological deficits but also the resultant socio-economic stresses that drive the demand for such interventions. More specifically, stress is a quantifiable deviation from the baseline values, which indicates unfavorable conditions. Hydrological stress is the shortfall in rainfall relative to the baseline, while social stress is the excess poverty above the baseline. Together, these stresses capture the compounded environmental and socio-economic pressures driving irrigation need.

Decades of research have extensively documented the physical dimensions of water scarcity in Sub-Saharan Africa and other global regions [8, 9]. Hydrologists and climatologists have developed sophisticated models to predict rainfall patterns, quantify water availability, and project future hydrological conditions under various climate change scenarios [10, 11]. Studies on drought indices, water balance models, and remote sensing of vegetation health have provided invaluable insights into the biophysical manifestations of hydrological stress [12, 13]. Furthermore, the link between agricultural productivity and rainfall has been rigorously investigated, leading to advancements in drought-resistant crop varieties and water-efficient farming practices [14, 15]. Simultaneously, economists and development practitioners have explored the nature of poverty, looking into its drivers, indicators, and spatial distributions. Quantitative methods, including poverty mapping and household surveys, have allowed for a granular understanding of socio-economic vulnerability [16, 17]. Therefore, a robust body of knowledge has been established on both the environmental triggers of agricultural distress and the socio-economic indicators of human hardship. These two domains have largely been explored in parallel, yielding specialized insights within their respective fields. There is no doubt in the literature that a feasible solution to climatic variability in SSA is investment in irrigation systems [18].

Research on irrigation demand and water resource management has traditionally emphasized biophysical factors such as rainfall variability, soil moisture, and crop water requirements [19, 20]. Models integrating hydrological stress typically use drought indices [12, 21], water balance calculations [13, 22] and remote sensing data [10, 23]; to predict irrigation needs and optimize resource allocation. These studies provide critical insights into the environmental drivers of irrigation demand but generally treat socio-economic factors as external or secondary considerations. Parallel to this, socio-economic research has extensively examined poverty dynamics, vulnerability mapping, and the social impacts of climate variability [2, 16, 17]. Quantitative methods including poverty mapping and household surveys have revealed spatial and temporal heterogeneity in social stress [3], highlighting that communities respond differently to hydrological shocks based on economic resilience and access to resources. However, these studies rarely translate socio-economic vulnerability directly into irrigation demand metrics. Recent advances recognize the importance of integrating socio-economic vulnerability into water management frameworks [7], and there are some works that propose composite indices combining environmental and social indicators to capture multidimensional stress [24, 25]. Yet, many existing approaches rely on aggregated or static data, consequently lacking continuous, time-resolved formulations that capture dynamic interactions between hydrological deficits and poverty outcomes. Moreover, spatial heterogeneity in irrigation needs is often inferred rather than explicitly modeled.

Despite this extensive individual exploration, a significant gap in the literature persists regarding the integrated, quantitative assessment of irrigation demand that explicitly and directly links hydrological stress to its resulting socio-economic consequences, particularly poverty. While it is implicitly understood that rainfall deficits can lead to poverty, and poverty necessitates intervention, few models provide a continuous, time-resolved, and spatially-aware measure of irrigation need that is directly driven by this coupled dynamic. Traditional approaches to assessing irrigation requirements often focus predominantly on biophysical parameters such as soil moisture deficits, crop water requirements, or surface water availability [19]. While crucial, these purely biophysical models often overlook the human dimension, failing to prioritize interventions where the societal impact, manifested as increased poverty, is most severe. There is a lack of robust frameworks that integrate the 'why' (socio-economic impact) with the 'what' (hydrological deficit) in a way that quantifies the urgency of irrigation. Furthermore, existing studies often rely on discrete, aggregated data points, limiting the ability to capture dynamic changes or pinpoint precise temporal or spatial hotspots of compounded stress. The dynamics of

how hydrological stress translates into human suffering, and how this suffering can then guide the allocation of critical resources like irrigation, remain largely unquantified in a comprehensive, integrated index.

Our methodology explicitly defines hydrological and social stresses as measurable deviations from baselines and combines them multiplicatively into an irrigation need index. This approach not only captures the compounded effect of environmental and socio-economic pressures but also offers a continuous temporal formulation that enables analysis of irrigation demand dynamics beyond static annual snapshots. Unlike existing models, the continuous-time interpolation facilitates cumulative burden assessments and more targeted policy diagnostics. While our current work does not empirically incorporate spatial heterogeneity due to data constraints, the mathematical formulation inherently allows for such extensions in future studies, which would be vital for geographically targeted irrigation planning. This comprehensive integration of hydrological and socio-economic factors into a single, policy-relevant index represents a novel contribution with practical implications for irrigation planning and climate adaptation strategies.

This study aims to develop and apply a novel quantitative framework for assessing irrigation demand in Malawi, moving beyond purely biophysical considerations to explicitly integrate the socio-economic impact of rainfall variability, specifically poverty outcomes. We seek to answer the fundamental question: How can we quantify irrigation need in a manner that directly reflects the severity of social stress induced by hydrological deficits? Our primary objective is to create an irrigation need index that is not merely a function of water availability, but a direct indicator of human vulnerability and the resulting urgency for intervention. We intend to establish a clear mathematical relationship where increased poverty, especially when compounded by rainfall shortfalls, directly elevates the calculated need for irrigation.

Our approach differentiates itself from previous studies by offering several key contributions. Firstly, we define hydrological stress and social stress (poverty deviation) as distinct yet interconnected quantifiable entities, allowing us to explicitly model their compounded effect. Our innovative irrigation need index (I_k) uniquely combines these two deviations multiplicatively, meaning that the urgency for irrigation is amplified when both rainfall is scarce and poverty is high. This moves beyond correlational observations to a quantifiable causal and quantifiable link. Secondly, we introduce a continuous temporal representation of irrigation need, allowing us to analyze cumulative stress over time and identify prolonged periods of heightened demand, rather than just isolated annual events. This continuity facilitates the calculation of total irrigation burden and average intensity. Thirdly, we extend this framework to introduce spatial heterogeneity (without validation), allowing for the identification of specific geographic areas within Malawi experiencing the most acute and compounded stress. This spatial dimension is critical for targeted policy interventions and efficient resource allocation. However, we only propose the mathematical methodology without empirical validation to narrow the scope of this study, and also to manage data unavailability constraints.

By grounding our irrigation need assessment in observable poverty outcomes, our methodology provides a more socially relevant and policy-actionable metric, ensuring that irrigation investments are directed where they can have the greatest humanitarian and developmental impact. This study is arranged as follows: section 1 provides the introduction, and section 2 presents the Methodology, with model validation detailed in section 2.2. The discussion of results and conclusion are in sections 3 and 4 respectively.

2. Methodology

The methodology adopted in this study offers a quantitative framework for assessing irrigation demand in Malawi by linking rainfall variability with poverty outcomes. We integrate hydrological and socio-economic data through a mathematically rigorous framework that captures the compounded effects of rainfall deficits and poverty deviations over time. By quantifying hydrological stress as the normalized shortfall of rainfall relative to a baseline and social stress as the positive deviation of poverty incidence above its historical norm, we construct an irrigation need index that explicitly links environmental triggers to human vulnerability. The model employs a multiplicative formulation to reflect the non-linear amplification of irrigation urgency when both stresses are present concurrently. Unlike conventional models that rely on static or aggregated datasets, we introduce continuous temporal interpolation, enabling the estimation of irrigation demand at finer temporal resolutions and facilitating the analysis of cumulative irrigation burdens over extended periods.

This approach allows policymakers and planners to detect periods of acute stress that may require prioritized intervention. Furthermore, the use of robust baseline definitions ensures that deviations are contextually meaningful and comparable across time. The methodology leverages publicly available climatic and poverty datasets, ensuring replicability and relevance to the Malawian context. While empirical validation is outside the scope of this study, the framework is designed for seamless integration with diverse data sources and can be extended to incorporate spatial heterogeneity in future work.

2.1 *The discrete and continuous frameworks*

The temporal domain is defined as a one-dimensional topological space $B = \{b_1,\ b_2,\ \ldots,\ b_k\}$, where each b_k corresponds to a calendar year from 2002 to 2022, giving a total of $k = 21$ segments. Each segment represents a distinct temporal observation during which annual environmental and socio-economic conditions are recorded. Rainfall and poverty are taken as the key indicators of hydrological conditions and social vulnerability, respectively. For each year k, the annual rainfall and poverty level are normalized to the unit interval $[0, 1]$ using min-max scaling. This yields two sequences: R_k representing normalized rainfall, and P_k representing normalized poverty levels, for $k = 1,\ 2,\ \ldots,\ 21$. The normalization ensures comparability of magnitudes across different years and permits a consistent treatment of deviation from optimal conditions.

To define reference baselines, we identify R^*, the maximum normalized rainfall over the 21-year period, and P^*, the minimum normalized poverty level during the same interval, under non-cyclonic conditions. These baselines are understood to represent optimal hydrological conditions and minimal social stress, respectively. Specifically, the baselines represent the optimal reference values against which current observations are compared. For rainfall, the baseline (R^*) is defined as the maximum normalized rainfall observed during the study period, representing ideal hydrological conditions. For poverty, the baseline (P^*) is the minimum normalized poverty level observed, reflecting minimal social stress. From these baselines, two deviation vectors are constructed. The rainfall deviation, or hydrological stress, is defined as

$$\Delta_k = R^* - R_k, \tag{1}$$

for each year k, and the poverty deviation, or social stress, is given by

$$\delta_k = P_k - P^*. \tag{2}$$

These deviation terms quantify how far each year's observed conditions diverge from their respective optimal states. The irrigation demand is conceptualized as a function of both these deviations, encapsulating the notion that irrigation is not merely a response to rainfall deficit but to its socio-economic consequences as reflected in poverty outcomes. To this end, an irrigation need index I_k is defined for each year k as follows:

$$I_k = \left(\frac{\delta_k}{P^* + \varepsilon}\right) \cdot (1 + \alpha\Delta_k), \tag{3}$$

where ε is a small positive constant introduced to ensure numerical stability in cases where P^* may approach zero, and α is a tunable parameter representing the sensitivity of the irrigation need to hydrological stress. The term $\dfrac{\delta_k}{(P^* + \varepsilon)}$ captures the proportionate rise in poverty above the ideal baseline, serving as a socially grounded signal of stress. The multiplicative adjustment $(1 + \alpha\Delta_k)$ amplifies the irrigation need in direct response to rainfall shortfall.

This formulation allows for the identification of critical years in which the compounded effects of rainfall deficit and poverty exceed tolerable thresholds, justifying irrigation intervention. The index I_k serves both diagnostic and predictive purposes, offering a time-resolved, data-driven measure of irrigation urgency that reflects both environmental and social

dimensions. To model the continuous case, we begin with the discrete sequence of irrigation need values $\{I_k\}$, defined annually over the interval $t_k \in \{2002,\ 2003,\ \ldots,\ 2022\}$. Each value I_k reflects the calculated irrigation requirement for year k, derived from the relative excess in poverty over its baseline and, optionally, modulated by deviations in rainfall. While this formulation is suitable for year-by-year analysis, it limits our ability to assess cumulative trends or continuous temporal stress. To overcome this, we seek a continuous representation of irrigation needs.

We define a continuous function $I(t)$ such that for each year t_k, we have

$$I_k \approx I(t_k), \tag{4}$$

where $I(t)$ is obtained via interpolation of the discrete values $\{I_k\}$. This transition enables us to consider irrigation need not only at discrete intervals but at any point within the time domain $t \in [2002,\ 2022]$. Interpolation of $I(t)$ is performed using a cubic spline method to ensure a smooth curve that closely fits the observed annual values I_k. This approach balances smoothness and accuracy, enabling continuous analysis over time. With a continuous function $I(t)$ defined, we quantify the total accumulated irrigation need over the full observation period. This is expressed as the definite integral of $I(t)$ with respect to time:

$$\mathscr{I} = \int_{t_0}^{t} I(t)dt. \tag{5}$$

This integral provides a scalar measure of the total irrigation burden sustained across the two-decade period. However, this cumulative measure does not convey the average intensity of irrigation pressure experienced annually. To obtain such a measure, we compute the mean value of the function $I(t)$ over the domain of interest:

$$\bar{I} = \frac{1}{t - t_0} \int_{t_0}^{t} I(t)dt. \tag{6}$$

The quantity $\bar{I}$ offers a normalized benchmark for comparing irrigation demand across regions or determining whether a particular year exceeds or falls below the long-term average. To identify intervals during which irrigation demand exceeds a policy-relevant threshold, we introduce a critical level Θ. We then define an indicator function $1_{\{I(t)>\Theta\}}$, which assumes the value 1 whenever the condition $I(t) > \Theta$ holds, and 0 otherwise. The total duration of such exceedance events is given by the integral

$$T_{\text{critical}} = \int_{t_0}^{t} 1_{I(t)>\Theta} dt. \tag{7}$$

This integral yields the total number of years, or fractional years in the case of continuous interpolation, during which irrigation need surpasses the critical threshold. It serves as a diagnostic tool for temporal targeting of irrigation infrastructure or emergency intervention.

We further extend this formulation to incorporate spatial heterogeneity. Let $x \in \Omega \subset \mathbb{R}$ denote a spatial coordinate over the national territory, and define $I(x,\ t)$ as the irrigation need at location x and time t. The total irrigation demand across space and time is then given by

$$\mathscr{I} * \Omega = \int_{t_0}^{t} \int_{\Omega} I(x,\ t)dxdt. \tag{8}$$

This formulation enables us to evaluate not only when but where irrigation demand is most acute, thereby informing geographically targeted investment and planning. By proceeding from discrete definitions to continuous representations, and subsequently to integrated forms, we establish a coherent framework for analyzing irrigation need. This continuous approach retains the social grounding of the original model, linking poverty to hydrological stress, while extending its applicability to dynamic and policy-relevant settings.

2.2 *Model validation*

To demonstrate the validity of this model empirically, we translate the theoretical constructs such as I_k and its continuous form $I(t)$ into computable metrics using available national-level data. This involves assembling temporal datasets, applying interpolation techniques, and performing numerical integration to reveal patterns of irrigation need over time. Although the full formulation of the model allows for spatial disaggregation, defining $I(x, t)$ using geolocated variables such as rainfall or poverty at the district level, this study does not implement spatial validation due to data limitations. As such, we adopt a national-scale analysis, treating Malawi as a single aggregated unit. Future work could extend this framework by applying it to district-level data, enabling geospatial mapping of irrigation need and more targeted intervention planning.

We structure the dataset such that for each year $t_k \in \{2002, \ldots, 2022\}$, we obtain measurements of normalized annual rainfall R_k, normalized poverty incidence P_k, and additional contextual variables such as Gross Domestic Product (GDP) and temperature. We source rainfall and temperature data from Google Earth Engine's Climate Hazards Center InfraRed Precipitation with Station data (CHIRPS) and Moderate Resolution Imaging Spectroradiometer (MODIS) repositories, respectively due to their long-term availability, spatial completeness, and relevance for climate-related agricultural assessment [26]. Poverty incidence data are retrieved from the World Bank, given its consistency and national coverage across the 21-year study period [27]. The resulting dataset comprises 21 annual observations per variable, structured as a time series for Malawi at the national scale. All variables are aggregated at the national level to maintain consistency and overcome limitations in the availability of high-resolution poverty data. We apply min-max normalization to the poverty data to rescale annual values into the unit interval, thereby enabling direct comparability with similarly normalized rainfall data. This normalization approach preserves relative year-to-year variation and ensures that deviations are computed on a consistent scale. However, we note that this method does not capture regional or demographic heterogeneity in poverty, which we acknowledge as a limitation of the current study. We anticipate that future implementations of this framework will incorporate disaggregated poverty metrics as such data become available.

We define the baseline reference values R^* as the maximum normalized rainfall observed over the study period and P^* as the minimum normalized poverty incidence. These values represent the most favorable hydrological and social conditions, respectively. From these baselines, we derive the rainfall deviation (Δ_k) and poverty deviation (δ_k), as given in Equations (1) and (2) respectively. These deviations quantify the annual shortfall from optimal rainfall and excess in poverty, respectively. We use these to define the irrigation need index for each year as

$$I_k = \left(\frac{\delta_k}{P^* + \varepsilon} \right) \times (1 + \alpha \Delta_k), \tag{9}$$

as given in Equation (3). The resulting function $I(t)$ enables numerical integration, temporal averaging, and the identification of exceedance periods. This trajectory is visualized in Figure 1.

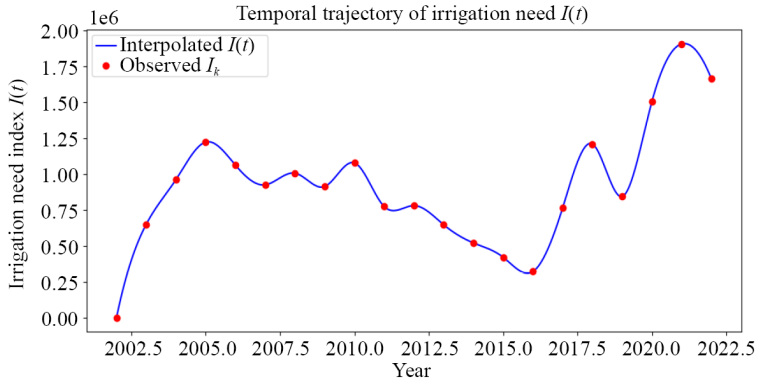

Figure 1. Temporal evolution of the irrigation need index $I(t)$ from 2002 to 2022. Red points show observed annual values I_k from rainfall and poverty deviations, while the blue curve is a cubic interpolation $I(t)$ that allows continuous analysis of irrigation demand over time

The observed annual irrigation need values (I_k) are depicted by the red points. These discrete data points are smoothed into a continuous function $(I(t))$ using a cubic interpolation, represented by the blue curve, which facilitates a temporal analysis of irrigation demand independent of the annual data collection points. Figure 2 displays $I(t)$ with the long-term average threshold $\Theta = \bar{I}$. Orange shading marks periods where demand exceeds Θ, totaling $T_{\text{critical}} = 10.47$ years, indicating sustained elevated irrigation need. This highlights critical intervals for policy attention. Figure 3 compares poverty levels by exceedance status, showing higher poverty rates during years when $I_k > \Theta$. Box plots and mean values with confidence intervals confirm the model's link between irrigation demand and socio-economic vulnerability.

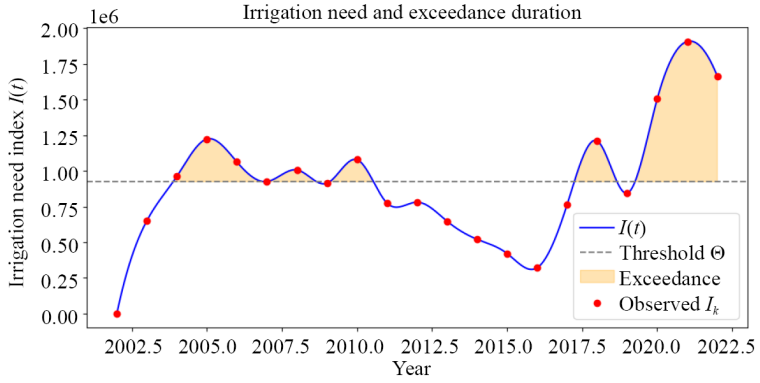

Figure 2. The plot shows the irrigation need index $I(t)$ from 2002 to 2022, with exceedance periods (where $I(t) > \Theta$) shaded in orange. Observed values I_k are marked in red, the interpolated curve is in blue, and the threshold Θ represents the long-term average. The total exceedance duration T_{critical} is calculated numerically

The average irrigation demand $\bar{I}$ over the entire period is used as the threshold Θ, representing a policy-relevant benchmark for irrigation demand. This allows the identification of periods when the instantaneous demand $I(t)$ exceeds Θ, to guide policy decisions or interventions. In Figure 2, we plot the temporal trajectory of $I(t)$ as a line chart, annotate it with critical thresholds Θ, and shade exceedance intervals corresponding to $T_{\text{critical}} = 10.47$ years. This suggests that for more than half of the 2002-2022 period, irrigation needs exceeded the average level, reflecting growing climatic variability or increasing pressure on water resources.

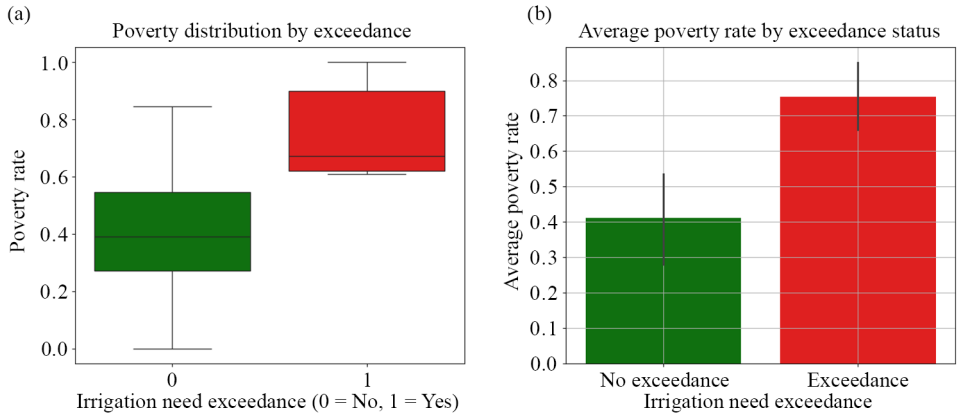

Figure 3. Poverty rate comparison by irrigation need exceedance status. (a) Box plot showing the distribution of normalized poverty rates for years classified by exceedance ($I_k > \Theta$). (b) Bar plot of the mean poverty rate with 95% confidence intervals, grouped by exceedance status. The plots are based on the classification threshold $\Theta = \bar{I}$

We construct a binary exceedance indicator to classify each year according to whether the irrigation need index I_k surpasses the threshold $\Theta = \bar{I}$ in Figure 3. Using this classification, we build a new data frame containing the normalized poverty rate and exceedance status for each year in the time series. We then generate two comparative visualizations. First, we use a box plot to display the distribution of poverty rates for the two exceedance groups: years with $I_k > \Theta$ and years with $I_k \leq \Theta$. Second, we compute and plot the mean poverty rate for each group using a bar plot with 95% confidence intervals. Both plots employ a consistent colour scheme, with green indicating non-exceedance and red indicating exceedance.

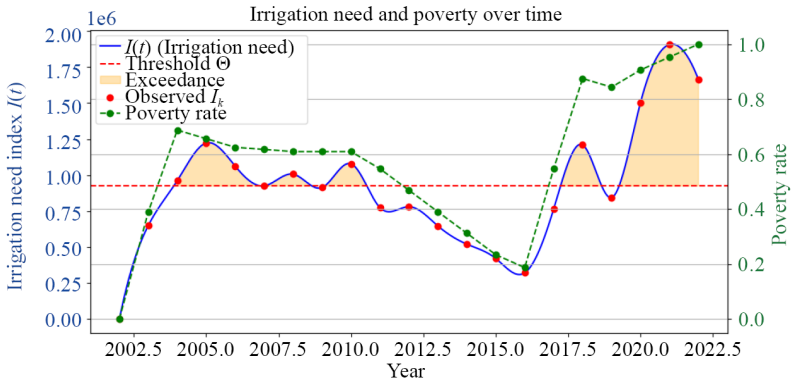

Figure 4. Temporal plot of the irrigation need index $I(t)$ and poverty rate from 2002 to 2022. The primary y-axis (left) displays the smoothed irrigation index $I(t)$ (blue), with red dots marking observed annual values I_k. The dashed red line indicates the threshold $\Theta = \bar{I}$, and orange shading highlights exceedance intervals where $I(t) > \Theta$. The secondary y-axis (right) shows the normalized poverty rate (green dashed line with markers). This dual-axis plot enables a joint view of irrigation stress and poverty conditions over time

In Figure 4, we overlay the interpolated irrigation need index $I(t)$ with poverty rate data to examine their temporal alignment. The function $I(t)$ is plotted as a smooth blue curve across the interval $[2002, 2022]$, with the policy-relevant threshold $\Theta = \bar{I}$ marked as a dashed red horizontal line. Exceedance regions, where $I(t) > \Theta$, are shaded in orange to visually indicate periods of elevated irrigation stress. Observed annual index values I_k are plotted as red dots. A secondary y-axis is added to display the normalized poverty rate, shown as a dashed green line with circular markers. This dual-axis visualization is constructed using a shared x-axis (Year) and enables simultaneous interpretation of irrigation need and poverty dynamics over time. Axis colours and labels are matched to their respective data series for clarity.

To demonstrate total irrigation demand over the full period, we compute integrals numerically:

$$\mathscr{I} = \int_{2002}^{2022} I(t)dt \approx \sum_{k=1}^{21} I_k \cdot \Delta t, \tag{10}$$

where $\Delta t = 1$ year, assuming a Riemann sum approximation. We calculate the cumulative exceedance by integrating the excess irrigation need above the threshold over time, which reflects the accumulated pressure on the system. We then compare this cumulative exceedance to a predefined investment threshold, which represents the critical level beyond which intervention becomes necessary.

To communicate the risk levels visually, we define three zones: a safe zone where the cumulative exceedance remains below half of the investment threshold, a caution zone where it lies between half and the full threshold, and a critical zone where it surpasses the investment threshold. These zones are shaded respectively in green, orange, and red to indicate increasing urgency in Figure 5. When the cumulative exceedance crosses the investment threshold, we mark the corresponding time point, and if the critical zone is exceeded, we annotate the plot to emphasize the necessity of investment. This approach allows us to assess the timing and severity of exceedance in a continuous manner, guiding informed decisions about infrastructure investment.

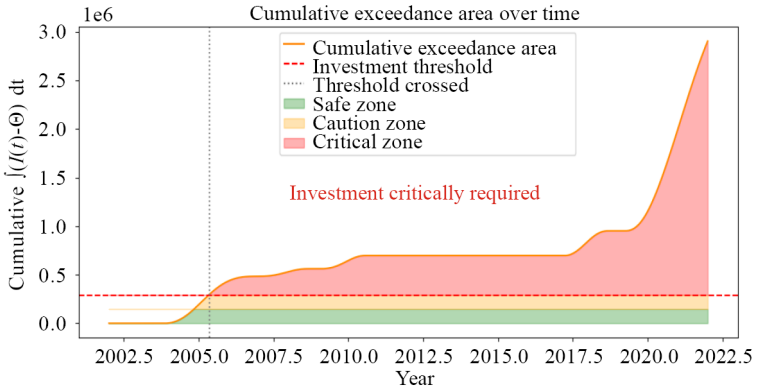

Figure 5. Cumulative exceedance area of irrigation need above the threshold over time. The green, orange, and red shaded regions represent safe, caution, and critical zones, respectively, defined relative to the investment threshold. The vertical dashed gray line indicates the time when the cumulative exceedance first crosses the investment threshold, signaling the point at which investment in irrigation infrastructure becomes critically required

We perform a Rainfall-Poverty quadrant analysis by classifying each year based on normalized rainfall and poverty relative to their mean values.

This divides observations into four quadrants: favourable (high rainfall, low poverty), water-stressed (low rainfall, low poverty), critical (low rainfall, high poverty), and inequity-risk (high rainfall, high poverty). Assigning years to these quadrants highlights periods where hydrological and social stresses coincide, particularly in the critical quadrant, indicating priority areas for irrigation investment.

The analysis in Figure 6 and Table 1 shows a worsening trend from 2020 to 2022, with most years in the critical quadrant and irrigation needs exceeding thresholds by 30%-45%. Repeated years in the inequity-risk quadrant reveal that water availability alone does not alleviate poverty, pointing to gaps in governance and infrastructure. Key insights include increased urgency since 2015, prioritizing persistent hotspots, and leveraging favourable periods for resilience building. This framework integrates poverty considerations into irrigation planning, directly informing investment and policy decisions.

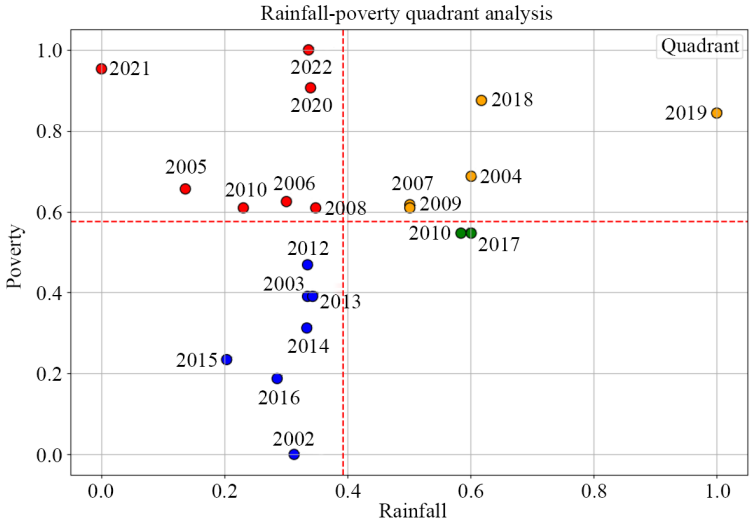

Figure 6. Quadrant classification of annual observations based on normalized rainfall and poverty levels. The horizontal and vertical lines represent the mean values of poverty and rainfall, respectively, dividing the plot into four zones: favorable (high rainfall, low poverty), water-stressed (low rainfall, low poverty), inequity-risk (high rainfall, high poverty), and critical (low rainfall, high poverty)

Table 1. Key years categorized by rainfall and poverty quadrants

Quadrant	Position years	Implications for irrigation investment
Critical (Low Rainfall, High Poverty)	2005, 2006, 2008, 2010, 2020-22	Significant need for urgent irrigation investment to alleviate vulnerability and improve resilience against water scarcity.
Inequity Risk (High Rainfall, High Poverty)	2004, 2007, 2009, 2018-19	Need for targeted investment to address systemic issues and improve water management, ensuring communities benefit from available resources.
Water-Stressed (Low Rainfall, Low Poverty)	2002, 2003, 2012-16	Lower urgency for investment, but opportunities to strengthen existing irrigation systems for future stability.
Favourable (High Rainfall, Low Poverty)	2017, 2010, 2011	Less immediate need for investment; potential to leverage high rainfall periods to build infrastructure for future challenges.

From Table 1, years in the Critical and Inequity-Risk quadrants reflect compounded hydrological and socio-economic stress. These periods may warrant prioritized intervention and targeted resource allocation.

3. Discussion

This study presents a novel quantitative framework for assessing irrigation demand in Malawi by integrating hydrological stress and socio-economic vulnerability into a unified irrigation need index. Unlike traditional approaches that rely primarily on meteorological data, our method explicitly combines rainfall deficits with deviations in poverty levels to capture the compounded impact of environmental and social stressors. By normalizing these indicators and defining baselines representing optimal conditions, we construct deviation metrics that inform an irrigation need index I_k, which amplifies urgency during years marked by simultaneous rainfall shortfalls and elevated poverty. The continuous-time formulation further enhances the framework by enabling smooth interpolation of annual data and supporting cumulative analyses, such as exceedance duration and long-term average irrigation demand. Although spatial disaggregation was proposed, data limitations restricted validation to the national scale; future studies can leverage higher-resolution socio-economic and climatic datasets to enable spatially explicit assessments.

Application of the model to Malawi over the 2002-2022 period reveals a significant increase in irrigation demand between 2020 and 2022, coinciding with documented declines in rainfall and rising poverty. This temporal trend reflects the increasing climatic variability and socio-economic pressures impacting smallholder farmers, emphasizing the need for adaptive water management strategies. The rising irrigation need during these years aligns with reports of droughts and food insecurity in Malawi, underscoring the practical relevance of integrating social vulnerability within irrigation planning frameworks. The tunable sensitivity parameter α provides flexibility for policymakers to adjust the index's responsiveness to hydrological stress, allowing the framework to be tailored to different risk tolerances or policy objectives. However, careful calibration alongside the stabilizing constant ε is necessary to prevent over-or under-estimation of irrigation urgency, ensuring that decisions are based on realistic and actionable thresholds. Sensitivity analysis of these parameters would be valuable in future work to optimize model performance.

The quadrant-based classification further elucidates the nuanced interplay between climate and poverty stress. Years classified in the Critical quadrant (for example, 2020-2022) highlight periods of compounded vulnerability where irrigation need is most acute, signaling urgent intervention requirements. This identification of high-risk periods can guide resource allocation to maximize impact and reduce socio-economic hardship. Meanwhile, the recurrence of Inequity-Risk years (for example, 2004, 2007, 2018-2019) emphasizes that adequate rainfall alone does not guarantee improved livelihoods, often due to governance and distributional inefficiencies. This finding draws attention to the importance of complementary policies addressing social equity and infrastructure distribution in parallel with irrigation development. In contrast, Water-Stressed years demonstrate scenarios where poverty mitigation occurs despite low rainfall, potentially reflecting effective infrastructure or adaptive capacity. Understanding these conditions can inform resilience-building measures and identify successful practices for scaling. The rarity of Favorable years underscores the importance of leveraging such periods for resilience-building efforts and proactive planning.

Limitations of this study include the use of normalized, annual poverty data aggregated at the national level, which may mask important sub-national and intra-annual heterogeneity. Threshold definitions based on means may oversimplify complex nonlinear dynamics and temporal lags between environmental stressors and socio-economic outcomes. Furthermore, while a small stabilizing constant ε is incorporated to avoid numerical instability when baseline poverty P^* approaches zero, the model does not explicitly quantify uncertainty or measurement errors in poverty data, which could propagate through the irrigation need index and influence the robustness of results. Future research should consider incorporating confidence intervals, sensitivity analyses, or probabilistic frameworks to better address these uncertainties. The potential impact of lag effects between rainfall deficits and poverty changes also warrants exploration to improve model accuracy. Future extensions could also incorporate dynamic thresholding and additional socio-economic indicators such as food insecurity, asset ownership, and access to services, enriching the framework's comprehensiveness.

4. Conclusion

This study advances irrigation planning by embedding social vulnerability into hydrological assessments, providing a dynamic, policy-relevant index that integrates environmental and socio-economic dimensions of irrigation demand. Our findings demonstrate the framework's ability to detect critical periods of compounded stress, offering actionable insights for prioritizing irrigation investments in Malawi. The flexible, continuous-time approach supports monitoring both gradual trends and acute events, enhancing decision-making for equitable and effective water resource management. Moving forward, incorporating spatial disaggregation and uncertainty quantification will be critical for improving the model's applicability and robustness. Strengthening water governance, ensuring equitable access, and fostering multi-sectoral coordination remain essential complements to infrastructure development. As climate variability intensifies and socio-economic vulnerabilities persist, integrated approaches such as ours will be vital for sustainable and inclusive irrigation policy in agriculture-dependent low-income contexts.

Authors contributions

All authors contributed equally to the writing of this paper. All authors read and approved the final manuscript.

Funding sources

This research did not receive any specific grant from funding agencies in the public, commercial, or not-for-profit sectors.

Conflict of interest

The authors declare no competing financial interest.

References

[1] Olayide OE, Alabi T. Between rainfall and food poverty: Assessing vulnerability to climate change in an agricultural economy. *Journal of Cleaner Production*. 2018; 198: 1-10. Available from: https://doi.org/10.1016/j.jclepro.2018.06.221.

[2] Beyene SD. The impact of food insecurity on health outcomes: Empirical evidence from sub-Saharan African countries. *BMC Public Health*. 2023; 23(1): 338. Available from: https://doi.org/10.1186/s12889-023-15244-3.

[3] Giller KE. The food security conundrum of sub-Saharan Africa. *Global Food Security*. 2020; 26: 100431. Available from: https://doi.org/10.1016/j.gfs.2020.100431.

[4] Iglesias A, Garrote L. Adaptation strategies for agricultural water management under climate change in Europe. *Agricultural Water Management*. 2015; 155: 113-124. Available from: https://doi.org/10.1016/j.agwat.2015.03.014.

[5] Higginbottom TP, Adhikari R, Dimova R, Redicker S, Foster T. Performance of large-scale irrigation projects in sub-Saharan Africa. *Nature Sustainability*. 2021; 4: 501-508. Available from: https://doi.org/10.1038/s41893-020-00670-7.

[6] Bjornlund V, Bjornlund H, van Rooyen AF. Exploring the factors causing the poor performance of most irrigation schemes in post-independence sub-Saharan Africa. *International Journal of Water Resources Development*. 2020; 36(1): 54-101. Available from: https://doi.org/10.1080/07900627.2020.1808448.

[7] Nhamo L, Mpandeli S, Liphadzi S, Dirwai TL, Mugiyo H, Senzanje A, et al. Why do farmers not irrigate all the areas equipped for irrigation? Lessons from southern Africa. *Agriculture*. 2024; 14(8): 1218. Available from: https://doi.org/10.3390/agriculture14081218.

[8] Hannemann M. *The Sub-Saharan water crisis: An analysis of its impact on public health in urban and rural Nigeria*. Honor Scholar Thesis. Greencastle, IN, USA: DePauw University; 2015.

[9] Nyika J, Dinka MO. Water challenges in rural sub-Saharan Africa. In: *Water Challenges in Rural and Urban Sub-Saharan Africa and Their Management*. Cham: Springer; 2023. p.39-55.

[10] Worku G, Teferi E, Bantider A, Dile YT. Modelling hydrological processes under climate change scenarios in the Jemma sub-basin of upper Blue Nile Basin, Ethiopia. *Climate Risk Management*. 2021; 31: 100272. Available from: https://doi.org/10.1016/j.crm.2021.100272.

[11] Banda VD, Dzwairo RB, Singh SK, Kanyerere T. Hydrological modelling and climate adaptation under changing climate: A review with a focus in sub-Saharan Africa. *Water*. 2022; 14(24): 4031. Available from: https://doi.org/10.3390/w14244031.

[12] Alito KT, Kerebih MS, Hailu DA. Characterization of drought detection with remote sensing based multiple indices and SPEI in northeastern Ethiopian highland. *Air, Soil and Water Research*. 2025; 18: 11786221251328833. Available from: https://doi.org/10.1177/11786221251328833.

[13] Sseguya F, Jun KS. Drought quantification in Africa using remote sensing, Gaussian kernel, and machine learning. *Water*. 2024; 16(18): 2656. Available from: https://doi.org/10.3390/w16182656.

[14] Wang L, Ren W. Drought in agriculture and climate-smart mitigation strategies. *Cell Reports Sustainability*. 2025; 2(6): 100386. Available from: https://doi.org/10.1016/j.crsus.2025.100386.

[15] Orimoloye IR. Agricultural drought and its potential impacts: Enabling decision-support for food security in vulnerable regions. *Frontiers in Sustainable Food Systems*. 2022; 6: 838824. Available from: https://doi.org/10.3389/fsufs.2022.838824.

[16] Tennant E, Ru Y, Sheng P, Matteson DS, Barrett CB. Microlevel structural poverty estimates for southern and eastern Africa. *Proceedings of the National Academy of Sciences of the United States of America*. 2025; 122(6): e2410350122. Available from: https://doi.org/10.1073/pnas.2410350122.

[17] Steele JE, Sundsøy PR, Pezzulo C, Alegana VA, Bird TJ, Blumenstock J, et al. Mapping poverty using mobile phone and satellite data. *Journal of the Royal Society Interface*. 2017; 14(127): 20160690. Available from: https://doi.org/10.1098/rsif.2016.0690.

[18] Hanjra MA, Williams TO. Global change and investments in smallholder irrigation for food and nutrition security in sub-Saharan Africa. In: Gomez y Paloma S, Riesgo L, Louhichi K. (eds.) *The Role of Smallholder Farms in Food and Nutrition Security*. Cham: Springer; 2020. p.99-131.

[19] Ahmed Z, Gui D, Murtaza G, Yunfei L, Ali S. An overview of smart irrigation management for improving water productivity under climate change in drylands. *Agronomy*. 2023; 13(8): 2113. Available from: https://doi.org/10.3390/agronomy13082113.

[20] Sawadogo A, Dossou-Yovo ER, Kouadio L, Zwart SJ, Traoré F, Gündoğdu KS. Assessing the biophysical factors affecting irrigation performance in rice cultivation using remote sensing derived information. *Agricultural Water Management*. 2023; 278: 108124. Available from: https://doi.org/10.1016/j.agwat.2023.108124.

[21] Wang Y, Liu T, Duan L, Chu S, Sun J, Tong X, et al. A novel index combining meteorological, hydrological, and ecological anomalies used for ecological drought assessment at a grassland-type basin scale. *Ecological Indicators*. 2025; 173: 113384. Available from: https://doi.org/10.1016/j.ecolind.2025.113384.

[22] Wegehenkel M, Kersebaum KC. The validation of a modelling system for calculating water balance and catchment discharge using simple techniques based on field data and remote sensing data. *Physics and Chemistry of the Earth, Parts A/B/C*. 2005; 30(1-3): 171-179. Available from: https://doi.org/10.1016/j.pce.2004.08.023.

[23] Xu C, Han Z, Fu H. Remote sensing and hydrologic-hydrodynamic modeling integrated approach for rainfall-runoff simulation in farm dam dominated basin. *Frontiers in Environmental Science*. 2022; 9: 817684. Available from: https://doi.org/10.3389/fenvs.2021.817684.

[24] Rabiei-Dastjerdi H, Brereton F, O'Neill E. Towards designing a comprehensive composite index for social vulnerability to natural hazards in the big data era: Potential challenges and partial solutions. *Natural Hazards*. 2025; 121: 3885-3913. Available from: https://doi.org/10.1007/s11069-024-06874-w.

[25] Stevens SM, Joy MK, Abrahamse W, Milfont TL, Petherick LM. Composite environmental indices-A case of rickety rankings. *PeerJ*. 2023; 11: e16325. Available from: https://doi.org/10.7717/peerj.16325.

[26] Google Earth Engine Team. *Google Earth Engine Data Repository: CHIRPS and MODIS Collections*. 2024. Available from: https://developers.google.com/earth-engine/datasets [Accessed 12th July 2025].

[27] World Bank. *Malawi Poverty Incidence Data*. 2024. Available from: https://data.worldbank.org/country/malawi [Accessed 12th July 2025].